Scientific Research Report

A Novel Antimicrobial Hydrogel for the Management of Periodontal Diseases

Pauline Yang Wong [a], *Shane Soo* [a], *Edmund Soon-Chern Wong* [a], *Praveen Praveen* [b], *Peta Clode* [c], *Murray V. Baker* [b], *Victor Haruo Matsubara* [a*]

[a] *UWA Dental School, The University of Western Australia, Perth, Western Australia, Australia*
[b] *School of Molecular Sciences, The University of Western Australia, Perth, Western Australia, Australia*
[c] *Centre for Microscopy, Characterisation, and Analysis and School of Biological Sciences, The University of Western Australia, Perth, Western Australia, Australia*

ARTICLE INFO

Article history:
Received 30 November 2022
Received in revised form
29 December 2022
Accepted 3 January 2023
Available online 6 February 2023

Keywords:
Antimicrobial agent
Hydrogel
Silver nanoparticles
Chlorhexidine
Tissue scaffolds

ABSTRACT

Objectives: This study aimed to synthesise a drug-delivery system based on a porous polymer hydrogel, with antimicrobial properties against *Porphyromonas gingivalis* and potential to be used in tissue regeneration.

Material and methods: 2-Hydroxyethyl methacrylate monomers were polymerised using thermal and photoactivation in the presence of silver nitrate ($AgNO_3$) and/or chlorhexidine digluconate. Poly-2-hydroxyethyl methacrylate (pHEMA) hydrogels containing silver nanoparticles (*AgNPs*) and/or 0.12% chlorhexidine (*CHX*) were produced and characterised using cryo-SEM and confocal microscopy. Hydrogel degradation and leaching of *AgNP* were tested for 1.5 months. The antimicrobial properties were tested against *P. gingivalis* using broth culture system and disk diffusion tests.

Results: Our methodology manufactured porous polymeric hydrogels doped with *AgNPs* and *CHX*. Hydrogels showed a successful delivery of *CHX* and sustainable release of *AgNPs* in a steady hydrogel degradation rate determined based on the weight loss of samples. Hydrogels with *AgNPs* or *CHX* had a significant antimicrobial effect against *P. gingivalis*, with *CHX*-hydrogels exhibiting a stronger effect than *AgNP*-hydrogels in the short-term assessment. *AgNP-CHX* hydrogels showed a compounded antimicrobial effect, whereas control hydrogels containing neither *AgNPs* nor *CHX* had no influence on bacterial growth ($P < .05$).

Conclusions: The dual-cured pHEMA hydrogel loaded with antimicrobial agents proved to be an efficient drug-delivery system against periodontopathogens, with the potential to be used as a scaffold for tissue regeneration.

Introduction

Oral diseases, including periodontal and peri-implant diseases, have been classified as major public health issues due to their high prevalence worldwide.[1] The severe form of periodontitis affects approximately 11% of the global population,[2] whilst peri-implantitis appears in 20% of patients in the first 5 to 10 years of implant placement.[3] Despite the significant progress in regenerative periodontal therapies and an increased understanding of the pathophysiology of periodontal diseases, the conventional nonsurgical management of periodontitis has not evolved significantly over the last decade.[4,5] The long-term effectiveness of scaling and root

* *Corresponding author*. UWA Dental School, University of Western Australia, 17 Monash Avenue, Nedlands, Perth, WA 6009, Australia.
Pauline Yang Wong: http://orcid.org/0000-0001-9239-987X
Shane Soo: http://orcid.org/0000-0003-4296-6383
Edmund Soon-Chern Wong: http://orcid.org/0000-0003-2689-069X
Praveen Praveen: http://orcid.org/0000-0002-6011-2536
Peta Clode: http://orcid.org/0000-0002-5188-4737
Murray V. Baker: http://orcid.org/0000-0002-0482-3421
Victor Haruo Matsubara: http://orcid.org/0000-0003-3481-1621
https://doi.org/10.1016/j.identj.2023.01.002

debridement is affected by regrowth of pathogenic microorganisms[6] and their limited removal in deep subgingival pockets.[7] Therefore, adjunct antimicrobials have been suggested to improve treatment effectiveness,[7] but there are limitations to drug delivery with current topical antimicrobials.[8]

Chlorhexidine (*CHX*) and silver nanoparticles (*AgNPs*) have shown to be effective antimicrobials against various common periodontal and oral pathogens.[9-11] One product already available in the market is the PerioChip, which is a controlled-release biodegradable gelatin containing chlorhexidine digluconate. Despite effective levels of *CHX* being maintained in the gingival crevicular fluid over a week without systemic absorption,[12] the clinical benefit of this drug-delivery system remains controversial.[13,14]

Various potential drug-delivery techniques have been tested to deliver drugs directly into the gingival sulcus, including polymer hydrogels such as carboxymethyl cellulose, chitosan, and naturally derived polymers.[15,16] The hydrogel used in this manner must have favourable properties, including biocompatibility, biodegradability, and good mechanical integrity.[17]

Polymer hydrogels have also been used as a scaffold in tissue engineering where the presence of porosities is an essential property for cell adhesion and cell proliferation in tissue growth.[17] A previous study has created a poly(2-hydroxyethyl methacrylate)–based hydrogel doped with *AgNPs*, which presented a biocompatible porous structure with in vitro antimicrobial effects against *Escherichia coli* and *Staphylococcus aureus*.[18]

The mechanisms involved in the antimicrobial effect of *AgNPs* have not yet been fully elucidated. Observations showed that silver ions are able to affect different structures of bacterial cells,[19] increasing, for example, the permeability of membrane that leads to cell lysis.[20] *AgNPs* can also damage DNA, bacterial proteins,[21] and lipids.[22] *AgNPs* are considered biocompatible when utilised at an appropriate dosage, with no influence on cell differentiation, but an increase in cell stress and toxicity at higher concentrations.[23]

The development of a cost-effective drug-delivery system based on a porous hydrogel, which could also work as a scaffold for tissue regeneration, would be an important advancement in the management of periodontal diseases and peri-implantitis. Therefore, this study aimed to synthesise a novel polymer hydrogel presenting not only antimicrobial activity against periodontal pathogens but also properties required in a scaffold for tissue engineering applications. Antimicrobial activity was achieved by incorporating *CHX* and *AgNPs* into the hydrogel structure, and the hydrogel applicability was enhanced through a combination of photo- and thermally induced polymerisation.

Materials and methods

Materials

2-Hydroxyethyl methacrylate (HEMA; Sigma-Aldrich), 2,2-dimethoxy-2-phenylacetophenone (DPAP; Sigma-Aldrich), $AgNO_3$ (Lab Supply), chlorhexidine digluconate solution (Sigma-Aldrich), potassium persulfate (Unilab, Ajax Chemical Co. Pty Ltd.) were used without further purification. Ultrapure water was obtained from a Milli-Q system and used for sample preparation, storage, and inductively coupled plasma optical emission spectrometry (ICP-OES) studies.

Preparation of pHEMA hydrogels

Polymer hydrogels were prepared via both photo and thermal polymerisation of HEMA in aqueous solution as a modification of a previously described method.[18] DPAP was used as a photo activator and potassium persulfate as thermal activator. UV irradiation followed by incubation in water bath at 37 °C temperature was used to initiate the polymerisation reaction (Figure 1). A detailed description of hydrogel preparation is provided as Supplementary Material.

Four variations of the hydrogel formula were tested: *control* hydrogel—plain hydrogel with no addition of chlorhexidine digluconate (CD) or $AgNO_3$; *CHX* hydrogel—containing CD; *AgNP* hydrogel—containing $AgNO_3$; and *CHX-AgNP* hydrogel—containing both CD and $AgNO_3$. Once the polymerisation

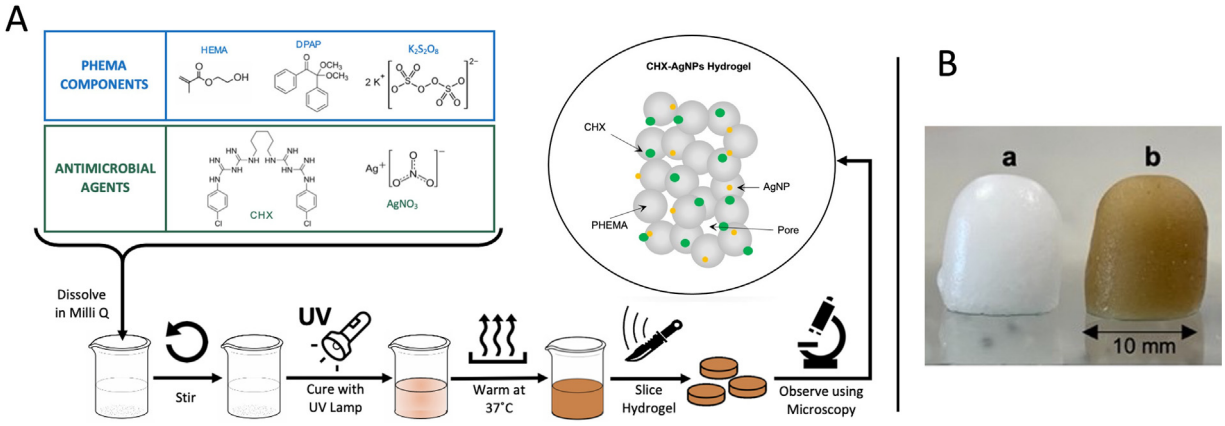

Fig. 1 – A, Formulation of pHEMA hydrogels doped with chlorhexidine (*CHX*) and silver nanoparticles (*AgNP*). B, Photograph of hydrogel samples: (a) control hydrogel and (b) *CHX-AgNP* hydrogel.

was completed, the hydrogels were carefully removed from vials (with the aid of a small spatula) and soaked in Milli-Q water for 12 hours to remove unreacted HEMA monomer.

Characterisation of pHEMA hydrogels

Cryo-scanning electron microscopy (cryo-SEM) and energy-dispersive x-ray spectroscopy (EDS) for hydrogel morphology analysis and silver identification

Hydrogel samples were sliced into pieces ~3 mm wide and ~0.5 mm thick, blotted on filter paper and mounted onto aluminium pins using optimal cutting temperature (OCT) compound, before being plunged frozen in liquid ethane (−180 °C; Leica, EM GP2). Frozen samples on pins were then loaded into a cryostage under liquid nitrogen and transferred under vacuum to the cryopreparation system (Leica, EM ACE600 + VCT500). Frozen samples were sublimated at −90 °C for 105 seconds to remove surface ice and reveal gel structure and then coated with 4 nm platinum. After coating, the samples were transferred under vacuum to the cryo-SEM (JEOL, IT800 field emission SEM + Leica, VCT500). Imaging was conducted at −155 °C and 10 kV using both secondary and backscattered electron signals. Qualitative element analysis and mapping of silver was performed at 10 kV using an x-ray detector interfaced to AZtec software (Oxford Instruments, 170 mm^2 Ultim® Max SDD EDS detector).

Confocal Raman spectroscopy for CHX *identification*

Raman spectra of *CHX*-containing hydrogels were collected using confocal laser Raman microscopy on a WITec alpha 300RA+ (WiTec) with a 532-nm laser source. The laser was focussed through a 100×/0.9 objective to obtain a spot size of smaller than 1 μm. Spectral acquisitions were obtained with 600 L mm^{-1} grating and a CCD detector peltier-cooled (−60 °C) with 1024×128 pixels. Laser centring and spectral calibration were performed daily on a silicon chip with characteristic Si Raman band of 520.4 cm^{-1}. Raman maps were acquired with a motorised stage allowing XYZ displacement with precision of better than 1 μm. The WITec Project FOUR software was used to analyse all spectra through background subtraction and peak fitting.

Degradation of pHEMA hydrogels in water

The mass loss of *CHX-AgNP* hydrogel was measured for 52 days, with samples incubated at 37 °C in aqueous solution at pH 6.8. The hydrogel samples were prepared by cutting the hydrogel with a razor blade into discs (10 mm diameter × 5 mm thick). The hydrogel dry mass was measured every 3 days (starting at day 0) after drying the samples for 40 minutes at 37 °C. At each assessment time point, 4 samples were dried and weighed using a digital laboratory scale.

ICP-OES to assess leaching of AgNPs

The leaching of *AgNPs* from hydrogels was evaluated over a 1.5-month period using an ICP-OES instrument (Agilent Technologies 5100, Agilent). *CHX-AgNP* hydrogel samples (15 mm thickness and 10 mm diameter) were transferred to centrifuge tubes containing 6 mL of ultrapure water immediately after the 12-hour washing period. Water was collected from each tube and replaced with fresh water (6 mL) every 3 days for 46 days. 70% Nitric acid (HNO_3,1 mL) was added to each sample, followed by sufficient ultrapure water to obtain a final volume of 10 mL.

All the sample solutions were filtered using nonpyrogenic 0.20-μm filters before injection into the ICP analysis system for Ag^+ analysis. Standard solutions with different Ag^+ concentrations were prepared from an Ag^+ standard solution (1000 ± 3 μg/mL) in 2% HNO_3 (from High-Purity Standards) by dilution in water. These solutions were used to generate a linear calibration curve (signal intensity as a function of concentration).

Antimicrobial tests against P. gingivalis

Strain and culture conditions

Gram-negative bacteria *P. gingivalis* (ATCC® 33277) was used as a periodontopathogen. The strain was grown under anaerobic conditions (90% N_2, 5% CO_2, and 5% H_2) at 37 °C on blood agar plates (TSA [Difco Laboratories] enriched with 5% defibrinated sheep blood, 0.5 mg/mL hemin [Sigma-Aldrich], and 1 mg/mL menadione [Sigma-Aldrich]). Enriched Tryptic Soy Broth (eTSB; yeast extract, hemin [5 mg/mL], and menadione [0.5 mg/mL]) was used for overnight growth.

Antibacterial activity of hydrogels within a broth culture system

The antibacterial effect of all 4 types of hydrogels doped with *CHX* and *AgNPs* was assessed using spectrophotometric semi-quantitative assay. After overnight bacterial growth in eTSB, the *P. gingivalis* suspension was adjusted to ~10^9 CFU/mL and 10 μL of this suspension was inoculated in 15 mL sterile centrifuge tubes with 4 mL of eTSB (2.5 × 10^6 UFC/mL final concentration). Polymer hydrogels (*control* hydrogel, *CHX* hydrogel, *AgNP* hydrogel, and *CHX-AgNP* hydrogel) were sliced with a razor blade into discs (10 mm diameter × 2 mm thick) and placed into tubes with *P. gingivalis* suspension (1 hydrogel type per tube). The mixtures were incubated at 37 °C for 48 hours.

Tubes containing polymer discs and bacterial suspension were examined after 24, 36, and 48 hours' incubation. At each assessment time, the optical density (OD) of each bacterial suspension was measured using a microplate reader (Tecan) at 600 nm. The percentage of *P. gingivalis* growth inhibition was calculated using the following formula:

$$\text{Percentage of inhibition}\,(\%) = 100\,\text{x}\,[1 - (\text{Sample OD} - \text{Medium OD})/(\text{Control OD} - \text{Medium OD})]$$

where Control OD is the absorbance of control hydrogel and Sample OD is absorbance of test hydrogels.

Disc inhibition assays

Hydrogels were sliced into discs 10 mm in diameter and 3 mm thick and placed onto blood agar plates inoculated with *P. gingivalis* and grown under anaerobic conditions at 37 °C for 5 days, followed by a qualitative analysis of the inhibition zones.

Statistical analysis

Nine samples per group were used for antimicrobial tests. The degradation test had 4 samples per reading. Data were presented as mean ± standard deviation (SD) from 3 independent experiments. One-way analysis of variance (ANOVA) followed by Tukey multiple comparison test was performed. Statistical significance was set at $P < .05$ (GraphPad Prism Version 6.0c—GraphPad Software).

Results

Hydrogel synthesis

The methodology developed in this study produced pHEMA hydrogels loaded with *CHX* and *AgNPs* using a dual-activation polymerisation reaction (Figure 1A). All hydrogel variations presented with a firm, sponge-like consistency after polymerisation (Figure 1B) except for the *CHX* hydrogels, which were slightly softer. The colour of the hydrogels varied based on antimicrobials incorporated. The *Control* and *CHX* hydrogels were white, the *AgNP* hydrogels were light brown, whilst *CHX-AgNP* hydrogels were darker brown.

Characterisation of hydrogels

Microscopy analyses

Cryo-scanning electron micrograph images showed that the pHEMA hydrogels loaded with both *AgNPs* and *CHX* presented morphologies based on a network of interconnected pores of dimensions 10 to 30 μm, which were distributed throughout the hydrogel sample (Figure 2). It is possible to identify fewer porosities on the hydrogel surface in contact with the cylindrical quartz vial (Figure 2A). Similar morphology was observed in the hydrogel without *AgNPs* and *CHX*. Under higher magnification, it is possible to visualise smaller holes (<10 μm) throughout that are ice crystal damage from freezing (Figure 2B), which is inevitable as freezing is part of the sample processing for cryo-SEM.

The back-scattered electron images from cryo-SEM showed abundant silver nanoparticles throughout the hydrogel and they were often clustered, forming larger particles (Figure 2C). When looking at isolated nanoparticles, it is possible to identify that some *AgNPs* synthesised during the hydrogel fabrication reaction presented a triangular shape, but most of them had rounded contour in a nanometre scale (Figure 2D).

Cryo-SEM and EDS analysis were used to evaluate the presence of *AgNPs* in hydrogel (Figure 2E, 2F). The energy-dispersive element mapping (Figure 2F) and the x-ray spectrum from the same area (Figure 2G) confirm the presence of Ag with Lα and Lβ Ag x-ray peaks being visible at 2.98 keV and 3.15 keV, respectively. Platinum peaks from the sample coating are also visible in the x-ray spectrum.

Confocal Raman spectroscopy confirmed the presence of *CHX* within *CHX-AgNP* hydrogel samples (Supplementary Material Figure 1).

Degradation of pHEMA hydrogels

The degradation of *CHX-AgNP* hydrogels was determined based on the weight loss of samples, which were incubated in water at 37 °C. On day 0 (immediately after synthesis), dry hydrogel discs weighed 202 mg on average. The hydrogels' weight was decreasing steadily over time, and at the end of the assessment period the average weight was 121 mg (Figure 3A). In 52 days, the hydrogel samples lost 40% of their dry weight, representing a significant degradation rate ($P < .0001$).

Leaching of AgNPs

CHX-AgNP hydrogels leached a significant amount of silver ions (approximately 30.7% of silver present in the initial formulation) during the first 7 days of incubation in water. Figure 3B shows a 4-day period of rapid leaching with the rate of leaching declining rapidly to almost zero by day 7. From day 10 onward, the silver leaching continues at a low rate until reaching zero at day 43.

Antimicrobial tests

A semi-quantitative analysis based on OD readings was used to assess the antimicrobial effect of hydrogels in a broth culture system. All hydrogels with antimicrobial agents significantly inhibited the growth of *P. gingivalis* at 24, 36, and 48 hours, especially the *CHX* and *CHX-AgNP* hydrogels ($P < .001$; Figure 4A). The control hydrogel showed no antimicrobial effect (Figure 4B), and its OD readings were higher than the test hydrogels for all readings taken. The percentage of bacterial growth inhibition (Table) was lower for *AgNP* hydrogel compared to *CHX* and *CHX-AgNP* in all time intervals. The antimicrobial effect of *CHX* and *CHX-AgNP* hydrogels were very similar, although *CHX-AgNP* hydrogel presented a slightly higher percentage of inhibition.

Control, *CHX*, and *CHX-AgNP* hydrogels were further investigated in a disc diffusion assay, which confirmed that the control hydrogel did not have antimicrobial effects. *CHX* and *CHX-AgNP* hydrogels had similar antimicrobial effects based on the inhibition zone around each sample (Figure 4C).

Discussion

A previous study from our group developed porous pHEMA sponges with antimicrobial capacity using a single-step methodology and light activation.[18] Based on this previous protocol, we have formulated a novel methodology to synthesise dual-cured polymeric hydrogels loaded with 2 important antimicrobial agents: *CHX* and *AgNPs*. The former is one of the most potent chemotherapeutic agent used in dentistry to control oral biofilms,[24] and the latter has been used in the medical field as an antimicrobial agent that promotes and accelerates the healing process.[25]

In terms of physical characteristics, our hydrogels containing *AgNPs* had a firmer consistency compared to hydrogels containing only *CHX*. It has been shown that the addition of *AgNPs* not only changes the colour of hydrogels but also accelerates polymerisation and affects the morphology of the resulting polymer.[18] In our pilot studies, higher

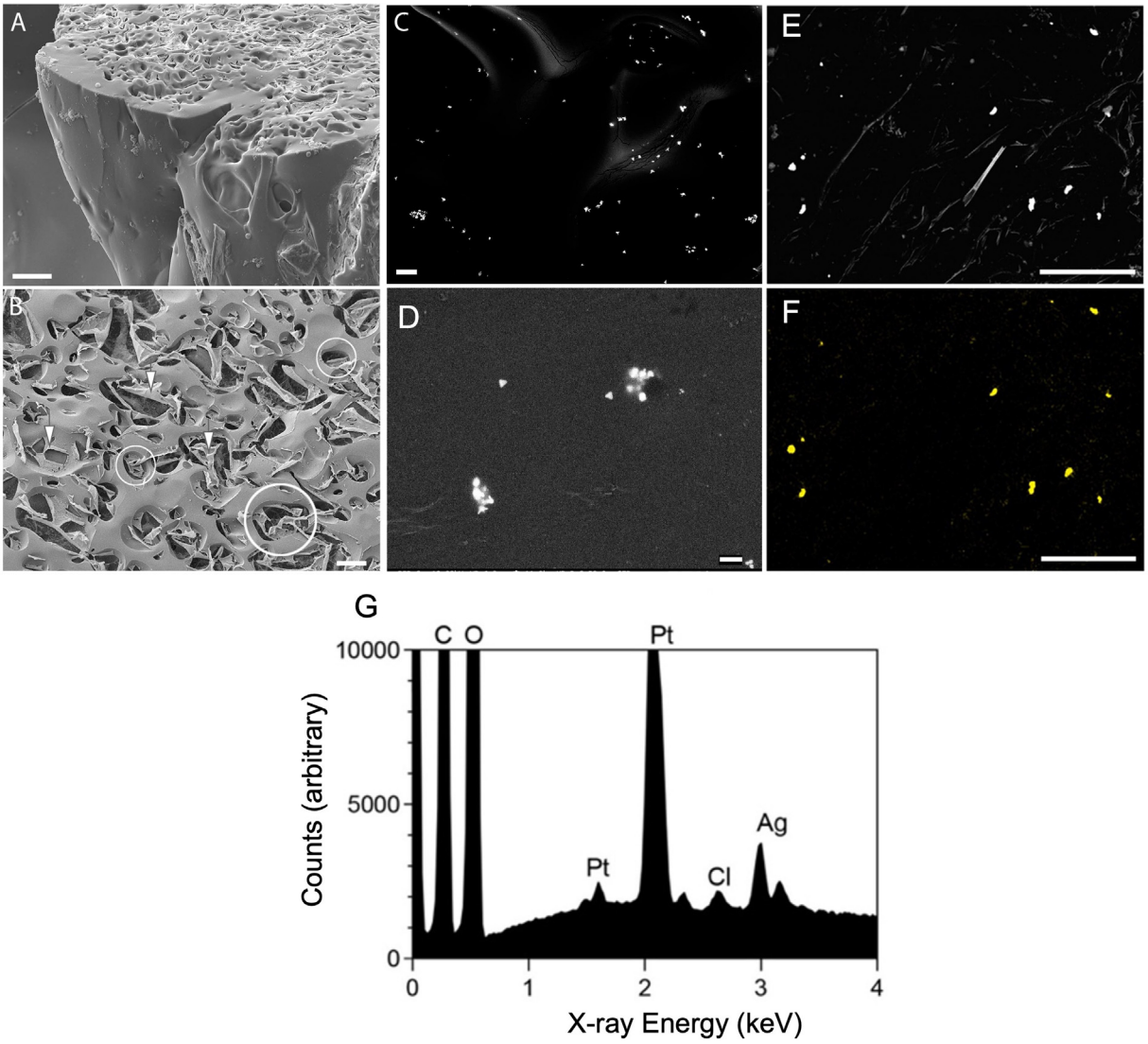

Fig. 2 – Cryo-scanning electron micrographs of hydrogel containing silver (Ag) particles. A, Low-magnification secondary electron image showing overall hydrogel structure. B, Secondary electron image showing pores of dimensions ~10–30 μm (eg, white circles) throughout the hydrogel. Some inevitable freezing damage (white arrows) is also evident. C, Back-scattered electron image showing abundant Ag nanoparticles throughout the hydrogel. D, Back-scattered electron image showing the shape of Ag nanoparticles. E, Back-scattered electron image showing region of analysis for element mapping. F, Element map of Ag from area depicted in (E), confirming bright features in back-scattered image are Ag particles. G, Energy-dispersive element analysis of silver nanoparticles in hydrogel, x-ray spectrum fxrom area depicted in (E) showing clear evidence of Ag with Lα and Lβ Ag x-ray peaks visible at 2.98 keV and 3.15 keV respectively. Scale bars = 50 μm (A), 10 μm (B), 2 μm (C), 1 μm (D), 25 μm (E and F).

concentrations of potassium persulfate displayed rapid polymerisation of hydrogel samples, but compromised synthesis of *AgNPs* within hydrogels. Therefore, the concentration of potassium persulfate was adjusted to allow sufficient time of UV light exposure to form *AgNPs* before completion of hydrogel polymerisation.

The *CHX-AgNP* hydrogel was found to be an efficient drug-delivery system, as it contained *CHX* in the form of chlorhexidine gluconate and sustained the release of *AgNPs* for more than a month. In contrast, previous experimental hydrogels containing *AgNPs* lost most of their silver content in the first 3 days postsynthesis.[26] The efficient and sustainable delivery of *CHX* and *AgNPs* promoted significant antimicrobial effect against *P. gingivalis*, an important periodontopathogen in the periodontal and peri-implant diseases. In our study, the antimicrobial tests demonstrated that both antimicrobial agents were responsible for the anti–*P. gingivalis* effect of the hydrogels. However, further studies on the duration of antimicrobial activity would need to be conducted to determine whether this sustained release of antimicrobials in the form of *CHX* and *AgNPs* would correspond to a similar length of antimicrobial activity. Even though the addition of *AgNPs* in

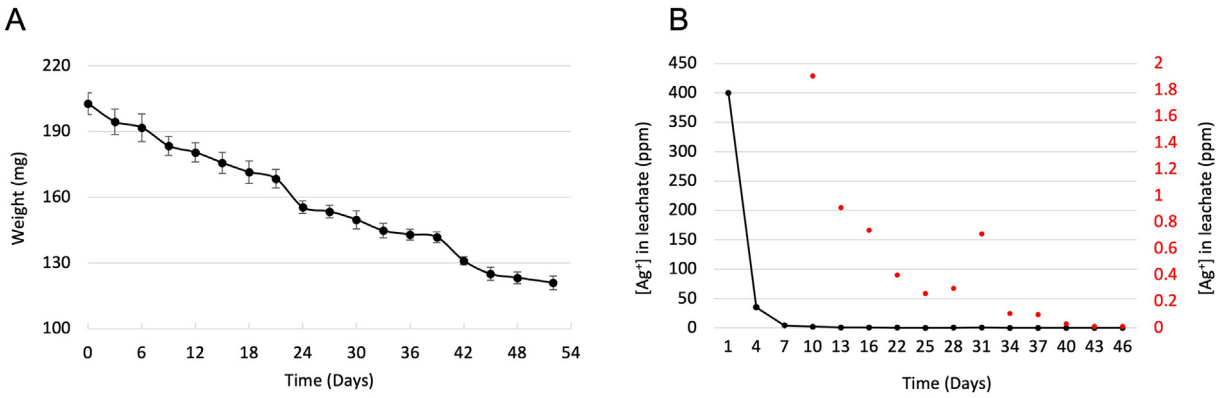

Fig. 3 – A, Amount of weight loss of hydrogels in aqueous solution at 37 °C. The mass loss of pHEMA hydrogels was measured for 52 days with samples kept in water. A steady hydrogel degradation rate was observed based on the continuous decrease in dry hydrogel weight over the degradation assessment period. B, Concentration of Ag^+ leached from *AgNP*-hydrogel. The points joined by the black line (reference to the concentration axis on the left) show a period of rapid leaching during the first 4 days with the rate of leaching declining rapidly to near zero by day 7. Data for day 10 onward (red points plotted on a magnified scale, concentration axis on the right) show that leaching continues at a low rate for many weeks until reaching zero at 43 days.

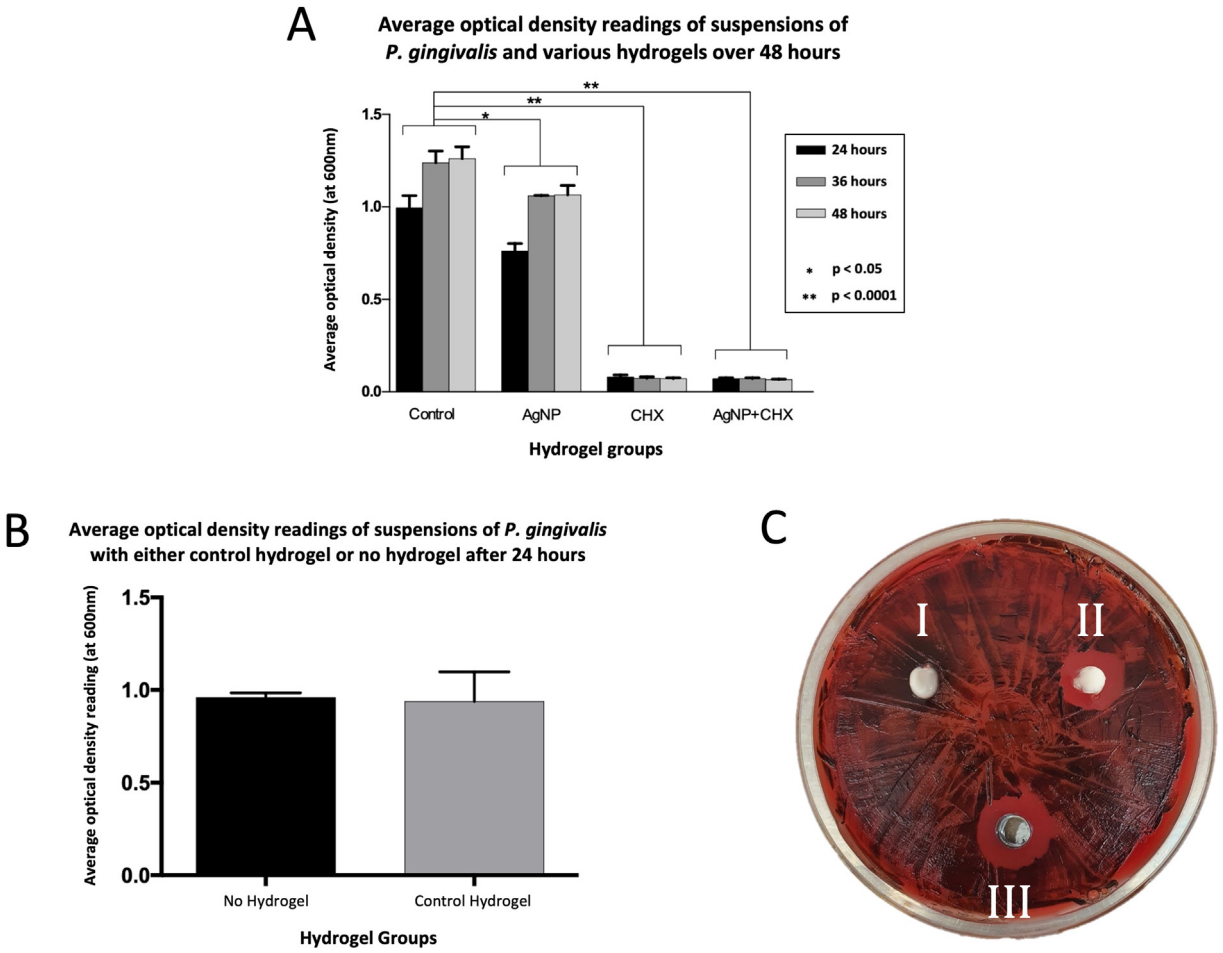

Fig. 4 – Antimicrobial activity of pHEMA hydrogels against planktonic *P. gingivalis* using broth culture assessment. A, Antibacterial activity of control hydrogel and test hydrogels evaluated after 24, 36, and 48 hours. B, Comparison between control hydrogel and broth culture with no hydrogel (positive control). Data are presented as mean ± SD. $^*P < .05$, $^{**}P < .001$. C, Disk diffusion test. Inhibition zone around pHEMA hydrogels against *P. gingivalis* after 5 days of incubation. I, Control; II, *CHX*; III, *AgNP-CHX* hydrogel.

Table – Percentage of bacterial growth inhibition promoted by hydrogels with antimicrobial activity against *P. gingivalis* after 3 different incubation periods.

Incubation time	Hydrogel		
	AgNP	*CHX*	*CHX-AgNP*
24 h	20	97	98
35 h	14	98	99
48 h	16	98	99

AgNP, silver nanoparticles; *CHX*, chlorhexidine.

the hydrogel formulation did not significantly increase the short-term antimicrobial effect of *CHX-AgNP* hydrogels compared to CHX hydrogels, the use of *AgNP* is believed to be beneficial for long-term antimicrobial effect due to the sustained release of *AgNPs*.

In contrast to existing drug delivery systems,[27] this new hydrogel formulation allows the synthesis of an antimicrobial scaffold within the periodontal defect, using a curing light source and body temperature to activate and accelerate *AgNP* formation and hydrogel polymerisation. Therefore, this drug delivery system could be individually synthesised for any periodontal or peri-implant defect to achieve intimate contact with tissues and increase its retention within the defect.

Additionally, cryo-SEM analysis showed *CHX-AgNP* hydrogels with a monolithic PHEMA structure exhibiting porosity, with pores having dimensions 10 to 30 μm, and mass-loss studies showed that the hydrogels degrade slowly over about 50 days in aqueous media at 37 °C. These traits suggest that the hydrogels have potential to act as a scaffold to support cell adhesion and growth. Previous studies found that the size of pores in scaffolds for tissue engineering influences the cell behaviour, such as cell proliferation, gene expression, and cartilage-like matrix deposition.[28] As our hydrogels presented relatively small pores, they are likely to provide more adhesion support for tissue cells, despite the reduced space for cell growth.[29] Cross-linkers were not used in our reaction; therefore, the hydrogel did not have a polymer droplet morphology like in previous study.[18]

Biodegradability and biocompatibility are essential properties in scaffolds used in tissue regeneration.[30] Our polymer hydrogels, which had no addition of cross-linkers, presented a favourable degradation rate in water at body temperature, thus indicating that it could be biodegradable in the oral environment. On the contrary, the previous study testing pHEMA sponges doped with *AgNPs* as antibacterial agents used the cross-linking agent EDGMA (ethylene glycol dimethacrylate) in the hydrogel formulation[18] and, therefore, degradability was not evidenced. In the same study,[18] hydrogels formulated with HEMA and $AgNO_3$ were shown to be nontoxic to human corneal epithelial cells. Our new formulation would require further cytotoxicity tests before its application in animal and clinical studies, as we have incorporated additional components to obtain dual (photo and thermal) activation of polymerisation.

Conclusions

A novel methodology was devised and successfully produced dual-cured pHEMA hydrogels loaded with antimicrobial agents. These hydrogels showed to be an efficient and effective drug-delivery system against *P. gingivalis*. The hydrogel has microporosities, is biodegradable, and exhibits promising potential as a scaffold for tissue regeneration when treating periodontal or peri-implant diseases.

Conflict of interest

None disclosed.

Acknowledgements

The authors acknowledge the facilities and the scientific and technical assistance of Microscopy Australia at the Centre for Microscopy, Characterisation & Analysis, The University of Western Australia, a facility funded by the University, State, and Commonwealth Governments. The authors also thank Dr Kate Shearston for the technical support in the UWA Dental School research laboratory as well as the Colgate Research Grant and the Australian Dental Research Foundation for their contributions and invaluable support for this study.

Author contributions

Pauline Wong, Shane Soo, and Edmund Wong contributed equally to this study.

Supplementary materials

Supplementary material associated with this article can be found in the online version at doi:10.1016/j.identj.2023.01.002.

REFERENCES

1. Petersen PE. The World Oral Health Report 2003: continuous improvement of oral health in the 21st century–the approach of the WHO Global Oral Health Programme. Community Dent Oral Epidemiol 2003;31(Suppl 1)):3–23. doi: 10.1046/j..2003.com122.x.
2. Frencken JE, Sharma P, Stenhouse L, Green D, Laverty D, Dietrich T. Global epidemiology of dental caries and severe periodontitis - a comprehensive review. J Clin Periodontol 2017;44 (Suppl 18)):S94–105. doi: 10.1111/jcpe.12677.
3. Mombelli A, Muller N, Cionca N. The epidemiology of peri-implantitis. Clin Oral Implants Res 2012;23(Suppl 6)):67–76. doi: 10.1111/j.1600-0501.2012.02541.x.
4. Kotsovilis S, Karoussis IK, Trianti M, Fourmousis I. Therapy of peri-implantitis: a systematic review. J Clin Periodontol 2008;35(7):621–9. doi: 10.1111/j.1600-051X.2008.01240.x.
5. Larsson L, Decker AM, Nibali L, Pilipchuk SP, Berglundh T, Giannobile WV. Regenerative medicine for periodontal and peri-implant diseases. J Dent Res 2016;95(3):255–66. doi: 10.1177/0022034515618887.
6. Berezow AB, Darveau RP. Microbial shift and periodontitis. Periodontol 2000 2011;55(1):36–47. doi: 10.1111/j.1600-0757.2010.00350.x.
7. Lecic J, Cakic S, Janjic Pavlovic O, et al. Different methods for subgingival application of chlorhexidine in the treatment of patients with chronic periodontitis. Acta Odontol Scand 2016;74(6):502–7. doi: 10.1080/00016357.2016.1206964.

8. Scholz M, Reske T, Bohmer F, Hornung A, Grabow N, Lang H. In vitro chlorhexidine release from alginate based microbeads for periodontal therapy. PLoS One 2017;12(10):e0185562. doi: 10.1371/journal.pone.0185562.
9. Spacciapoli P, Buxton D, Rothstein D, Friden P. Antimicrobial activity of silver nitrate against periodontal pathogens. J Periodontal Res 2001;36(2):108–13. doi: 10.1034/j.1600-0765.2001.360207.x.
10. Matsubara VH, Igai F, Tamaki R, Tortamano Neto P, Nakamae AE, Mori M. Use of silver nanoparticles reduces internal contamination of external hexagon implants by *Candida albicans*. Braz Dent J 2015;26(5):458–62. doi: 10.1590/0103-644020130087.
11. Lecic J, Cakic S, Janjic Pavlovic O, et al. Different methods for subgingival application of chlorhexidine in the treatment of patients with chronic periodontitis. Acta Odontologica Scandinavica 2016;74(6):502–7. doi: 10.1080/00016357.2016.1206964.
12. Soskolne WA, Chajek T, Flashner M, et al. An in vivo study of the chlorhexidine release profile of the PerioChip in the gingival crevicular fluid, plasma and urine. J Clin Periodontol 1998;25(12):1017–21. doi: 10.1111/j.1600-051x.1998.tb02407.x.
13. Heasman PA, Heasman L, Stacey F, McCracken GI. Local delivery of chlorhexidine gluconate (PerioChip) in periodontal maintenance patients. J Clin Periodontol 2001;28(1):90–5. doi: 10.1034/j.1600-051x.2001.280114.x.
14. Daneshmand N, Jorgensen MG, Nowzari H, Morrison JL. Slots J. Initial effect of controlled release chlorhexidine on subgingival microorganisms. J Periodontal Res 2002;37(5):375–9. doi: 10.1034/j.1600-0765.2002.01003.x.
15. Rajeshwari HR, Dhamecha D, Jagwani S, et al. Local drug delivery systems in the management of periodontitis: a scientific review. J Control Release 2019;307:393–409. doi: 10.1016/j.jconrel.2019.06.038.
16. Soskolne WA, Heasman PA, Stabholz A, et al. Sustained local delivery of chlorhexidine in the treatment of periodontitis: a multi-center study. J Periodontol 1997;68(1):32–8. doi: 10.1902/jop.1997.68.1.32.
17. Ahmadi F, Oveisi Z, Samani SM, Amoozgar Z. Chitosan based hydrogels: characteristics and pharmaceutical applications. Res Pharm Sci 2015;10(1):1–16.
18. Praveen P, Suzuki S, Carson CF, et al. Poly(2-hydroxyethyl methacrylate) sponges doped with Ag nanoparticles as antibacterial agents. ACS Appl Nano Mater 2020;3(2):1630–9. doi: 10.1021/acsanm.9b02384.
19. Noronha VT, Paula AJ, Duran G, et al. Silver nanoparticles in dentistry. Dent Mater 2017;33(10):1110–26. doi: 10.1016/j.dental.2017.07.002.
20. Chaloupka K, Malam Y, Seifalian AM. Nanosilver as a new generation of nanoproduct in biomedical applications. Trends Biotechnol 2010;28(11):580–8. doi: 10.1016/j.tibtech.2010.07.006.
21. Feng QL, Wu J, Chen GQ, Cui FZ, Kim TN, Kim JO. A mechanistic study of the antibacterial effect of silver ions on *Escherichia coli* and *Staphylococcus aureus*. J Biomed Mater Res 2000;52(4):662–8. doi: 10.1002/1097-4636(20001215)52:4<662::aid-jbm10>3.0.co;2-3.
22. Inbakandan D, Kumar C, Bavanilatha M, Ravindra DN, Kirubagaran R, Khan SA. Ultrasonic-assisted green synthesis of flower like silver nanocolloids using marine sponge extract and its effect on oral biofilm bacteria and oral cancer cell lines. Microb Pathog 2016;99:135–41. doi: 10.1016/j.micpath.2016.08.018.
23. Pauksch L, Hartmann S, Rohnke M, et al. Biocompatibility of silver nanoparticles and silver ions in primary human mesenchymal stem cells and osteoblasts. Acta Biomater 2014;10(1):439–49. doi: 10.1016/j.actbio.2013.09.037.
24. Poppolo Deus F, Ouanounou A. Chlorhexidine in dentistry: pharmacology, uses, and adverse effects. Int Dent J 2022;72(3):269–77. doi: 10.1016/j.identj.2022.01.005.
25. Karade VC, Patil RB, Parit SB, Kim JH, Chougale AD, Dawkar VV. Insights into shape-based silver nanoparticles: a weapon to cope with pathogenic attacks. ACS Sustainable Chem Eng 2021;9(37):12476–507. doi: 10.1021/acssuschemeng.1c03797.
26. Boonkaew B, Suwanpreuksa P, Cuttle L, Barber PM, Supaphol P. Hydrogels containing silver nanoparticles for burn wounds show antimicrobial activity without cytotoxicity. J Appl Polym Sci 2013;131:40215. doi: 10.1002/app.40215.
27. Killoy WJ. The use of locally delivered chlorhexidine in the treatment of periodontitis. Clinical results. J Clin Periodontol 1998;25(11, Pt 2):953–8 discussion 78–9. doi: 10.1111/j.1600-051x.1998.tb02397.x.
28. Matsiko A, Gleeson JP, O'Brien FJ. Scaffold mean pore size influences mesenchymal stem cell chondrogenic differentiation and matrix deposition. Tissue Eng Part A 2015;21(3–4):486–97. doi: 10.1089/ten.TEA.2013.0545.
29. Han Y, Lian M, Wu Q, Qiao Z, Sun B, Dai K. Effect of pore size on cell behavior using melt electrowritten scaffolds. Front Bioeng Biotechnol 2021;9:629270. doi: 10.3389/fbioe.2021.629270.
30. Echeverria Molina MI, Malollari KG, Komvopoulos K. Design challenges in polymeric scaffolds for tissue engineering. Front Bioeng Biotechnol 2021;9:617141. doi: 10.3389/fbioe.2021.617141.